ISSN 0036-0244, Russian Journal of Physical Chemistry A, 2015, Vol. 89, No. 13, pp. 2492–2496. © Pleiades Publishing, Ltd., 2015.

PHOTOCHEMISTRY AND MAGNETOCHEMISTRY

Modification of Dense TiO_2 Particles Using Polyethylene Glycol Template: Synthesis, Characterization, and Photocatalytic Activity[1]

J. Dostanić[a], D. Lončarević[a], A. Radosavljević-Mihajlović[b], and D. M. Jovanović[a]

[a] *University of Belgrade, Institute of Chemistry, Technology and Metallurgy, Department of Catalysis and Chemical Engineering, Njegoševa 12, Belgrade, Serbia*

[b] *University of Belgrade, Institute of Nuclear Sciences Vinča, Laboratory for Material Science, P.O. Box 522, Belgrade, Serbia*

e-mail: jasmina@nanosys.ihtm.bg.ac.rs

Received January 12, 2015

Abstract—In this study, an effort has been made to prepare TiO_2 materials by sol–gel technique using polyethylene glycol (PEG) as pore directing agent. Different PEG amounts were used during samples preparation in order to investigate the change in intrinsic material properties. The photocatalytic activity of prepared catalysts was estimated by measuring the decomposition of arylazo pyridone dye. The optimum template amount was determined, resulting in catalyst with enhanced textural properties, optimal anatase/rutile ratio and hence improved photocatalytic properties. Specific surface area and anatase/rutile ratio were found to be the main contributing factors to the catalyst activity. A synergistic effect between anatase and rutile TiO_2 has been observed, since the presence of relatively inactive rutile phase enhanced the photoactivity of mixed TiO_2.

Keywords: titanium dioxide, polyethylene glycol, anatase, rutile, textural properties.

DOI: 10.1134/S0036024415130130

INTRODUCTION

In the last decades, heterogeneous photocatalysis using semiconductors has become an attractive method for the treatment of air and water pollution [1]. One of the most widely used and researched photocatalysts is TiO_2, due to its chemical stability, biocompatibility, physical, optical, and electrical properties. When TiO_2 is illuminated by light with photon energy equal to or greater than its band-gap energy (3.2 eV) the valence electrons excite to the conduction band resulting in generation of holes. The photo-generated electron/hole pairs can either recombine or migrate to the surface and initiate redox reactions. The photoactivity of TiO_2 depends on a number of parameters including the crystal structure [2], the ratio between anatase and rutile crystal phases, particle size distribution, specific surface area, mean pore size, structure defects on its surface and in bulk, etc. [3, 4]. The control of TiO_2 properties via alternative synthesis procedure is often used to provide catalyst with enhanced properties.

Among various methods for the synthesis of solid inorganic materials, the relatively simple and inexpensive sol–gel technique attracted considerable attention due to its possibility of deriving unique metastable structure at low reaction temperatures with excellent chemical homogeneity. In a typical sol–gel process, a colloidal suspension, or a sol, is formed from the hydrolysis, condensation and polymerization of the precursors. Despite many advantages offered by sol–gel technique, the method has some limitations, i.e. difficulty in controlling hydrolysis and condensation rate, which can lead to undesired decrease in surface area and porosity. In order to overcome these limitations many authors have used organic templates during catalyst synthesis, such as polyethylene glycol (PEG) [5–7], Pluronics triblock copolymer P123 [8, 9], polystyrene [10] or biocomposite gel [11] which decompose at high temperature resulting in porous structure formation.

In the current study different amounts of PEG (Mn = 200) were used to synthesize nanosized TiO_2 with appropriate microstructure characteristics and morphology. Despite the widespread use of PEG in TiO_2 synthesis, according to our knowledge, there is lack of studies that deal with PEG directing properties on structure-activity relationship. In this study the relationship between physicochemical properties and photoactivity of synthesized catalysts was discussed and the factor most influencing the photoactivity was established.

EXPERIMENTAL

15.3 mL of titanium isopropoxide (TTIP) were dissolved in 50 mL of anhydrous ethanol and 5.31 g of

[1] The article is published in the original.

Textural, structural and photocatalytic properties of TiO_2 catalysts

Sample	r[a]	S_{BET}[b] (m^2/g)	D_{max}[c] (nm)	V_{pore}[d] (mm^3/g)	Fraction of		Crystallite size		k_{app}[e] (h^{-1})	$k'_{app} \times 10^3$[f] ($g/m^2\ h$)
					anatase, %	rutile, %	anatase, %	rutile, %		
TiO_2	0	4.1	11.8	3.1	32.3	67.7	20.5	22.0	0.024	5.8
TiO_2/P1	0.5	5.3	13.1	12.3	24.3	75.7	22.1	27.0	0.032	6.1
TiO_2/P2	1	13.2	11.1	36.9	45.6	54.4	18.0	19.9	0.110	8.3
TiO_2/P3	2	17.4	11.6	45.0	51.3	48.6	19.0	25.5	0.203	11.6
TiO_2/P4	3	32.8	11.2	79.6	92.7	7.3	18.3	35.2	0.558	17.0
TiO_2/P5	5	43.1	12.5	102.9	100.0	0	18.2	–	0.680	15.8

[a] Molar ratio of PEG to TTIP.
[b] BET specific surface area.
[c] Average pore diameter determined by mercury porosimetry.
[d] Intraparticle pore volume determined by mercury porosimetry.
[e] Apparent first-order rate constant for arylazo pyridone dye decomposition.
[f] Apparent first-order rate constant per unit surface area for arylazo pyridone dye decomposition.

diethanolamine (DEA) at room temperature for 1h (solution A). DEA was used as a sol stabilizer, in order to restrain the rapid hydrolysis. Meanwhile, 125 mL of anhydrous ethanol were mixed with 14.4 mL of water and with appropriate amount of PEG, Mn = 200 (1.1, 2.2, 4.4, 6.6, or 11.0 g) to prepare solution B. Solution A was subsequently added dropwise to solution B under vigorous stirring for 30 min. The stabilized sol was aged for 12 h at room temperature followed by sol–gel conversion. After that, the gels were dried at 80°C for 12 h and finally calcined in air stream at 550°C with a heating rate of 3 K min^{-1} for 4 h. The synthesized samples were designated as TiO_2/PX, where X denotes different molar ratio of PEG to TTIP. For comparative study, the unmodified TiO_2 was prepared without template by the same sol–gel method.

Specific surface area of the samples (S_{BET}) was calculated from the nitrogen adsorption isotherms (Sorptomatic 1990 Thermo Finnigan automatic system), using nitrogen physisorption at –196°C according to the Brunauer, Emmett and Teller method [12]. Pore size, pore volume distribution, and porosity were determined by mercury intrusion porosimetry on Pascal 140/440, Thermo Scientific. Powder X-ray diffraction patterns were measured on a Rigaku diffractometer using CuK_α radiation. Diffuse reflectance UV–Vis (DR UV–Vis) spectra were recorded on Nicolet Evolution 500 spectrometer (Thermo Electron Corporation).

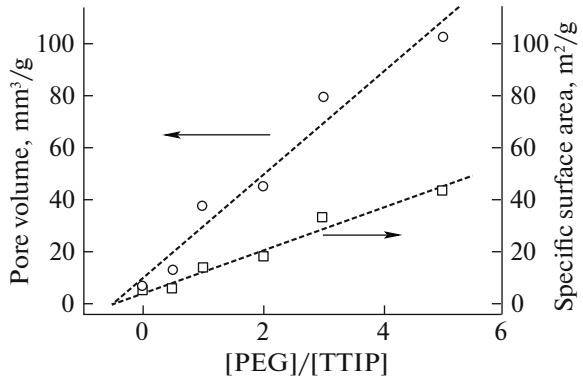

Fig. 1. Effect of PEG/TTIP molar ratio on pore volume and specific surface area of synthesized TiO_2 catalysts.

The photocatalytic activity of prepared catalysts was evaluated by decolorization of synthetic arylazo pyridone dye, 5-(4-sulfophenylazo)-6-hydroxy-4-methyl-3-cyano-2-pyridone [13] in an open cylindrical thermostatted Pyrex cell. The photocatalytic material (0.15 g) was dispersed in a dye solution (150 mL, 10 mg/L) using magnetic stirrer. The irradiation was performed using Osram Ultra Vitalux lamp (300W), which simulates solar radiation, housed 50 cm above the top surface of the dye solution. In order to remove the catalyst, after predetermined periods of time, the solution aliquots were centrifuged for 10 min at 17000 rpm, and analyzed by UV–Vis spectrophotometry (Thermo Electron Nicolet Evolution 500).

RESULTS AND DISCUSSION

Textural properties of the prepared catalysts are presented in the table. The obtained results clearly indicate that addition of PEG in preparation stage led to an improvement of porous structure of the unmodified sample; all modified samples have noticeably larger pore volume, porosity and surface area compared to the unmodified one.

As it was expected, the increase in the amount of PEG molecule led to increase in pore volume and specific surface area, without any significant change in pore diameter. Moreover, linear tendency (Fig. 1) regarding surface area/pore volume was observed with

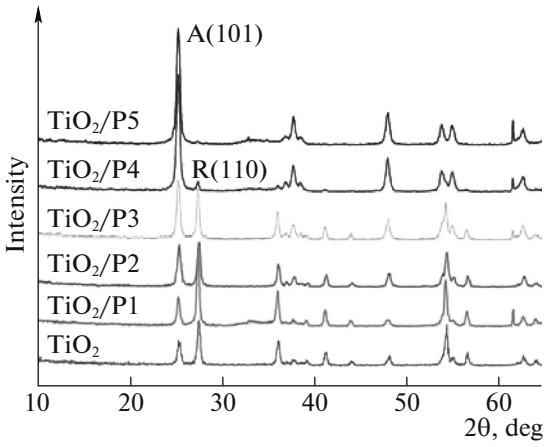

Fig. 2. XRD patterns of synthesized TiO_2 catalysts.

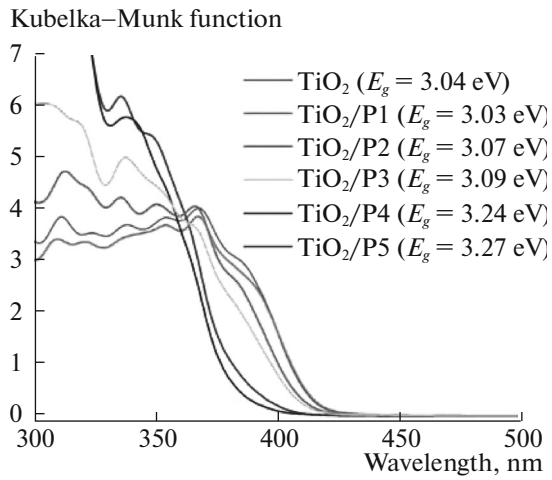

Fig. 3. UV–Vis diffuse-reflectance spectra of TiO_2 catalysts with determined band gap energies.

PEG increase, demonstrated that all PEG molecules participate in the formation of the TiO_2 network. Thus, among modified sample, the largest pore volume and specific surface area was obtained for the sample TiO_2/P5, prepared using the highest amount of PEG template.

The XRD patterns of synthesized catalysts are presented in Fig. 2. Diffraction peaks that correspond to anatase and rutile phases are marked with A and R, respectively. The main peaks are at 2θ angle of 25.2° and 27.3°, which are assigned to anatase (101) and rutile (110) crystalline phases, respectively. The phase content, defined as the percent of anatase phase in the samples, was determined from the ratio of peak heights in the XRD data according to the equation $F_A = 0.884I_A/(0.884I_A + I_R)$, where F_A presents fraction of anatase phase, I_A represents the intensity of anatase (101) peak, and I_R represents the intensity of the rutile (110) peak (table).

As can be seen from obtained results, the maximum rutile fraction was observed for control TiO_2 sample and modified TiO_2/P1 sample that was prepared using the smallest amount of PEG template. By increasing further the amount of the used PEG, the fraction of rutile phase decreases, while anatase phase becomes dominant. Thus, the sample TiO_2/P5, prepared using the highest amount of PEG template, consisted solely of anatase phase. It is interesting to note that crystalline structure among samples differs, although they were exposed to the same thermal treatment. As rutile nucleation may begin at the interparticle contact interface of anatase phase [14–16], the increase in PEG content and consequently decrease in interparticle contact prevents rutile nucleation at anatase twin interfaces.

The crystallite size of anatase and rutile phase was determined using Scherrer's equation (table). The results showed negligible difference between crystallite size among investigated catalysts. For a particular catalyst, rutile crystallite size was somewhat larger than that of anatase.

DR UV–Vis spectra of the samples are presented in Fig. 3. With increasing PEG content, the absorption edge shifts to higher energies. The band gap, E_g, of the samples was calculated applying Tauc plot [17] using Kubelka–Munk function for direct allowed transition (Fig. 3). The results show that PEG modification results in a blue shift of absorption edge from 3.04 to 3.27 eV. Among modified samples, the smallest band gap value of 3.03 eV was obtained for TiO_2/P1, while the highest value of 3.27 eV corresponds to TiO_2/P5. The determined band gaps of the samples are strongly related to the phase composition obtained from XRD measurements and reported band gap values for pure anatase (3.23 eV) and rutile phase (3.02 eV).

Photodegradation of arylazo pyridone dye using synthesized TiO_2 catalysts under simulated sunlight is presented in Fig. 4. Apparent first-order rate constants

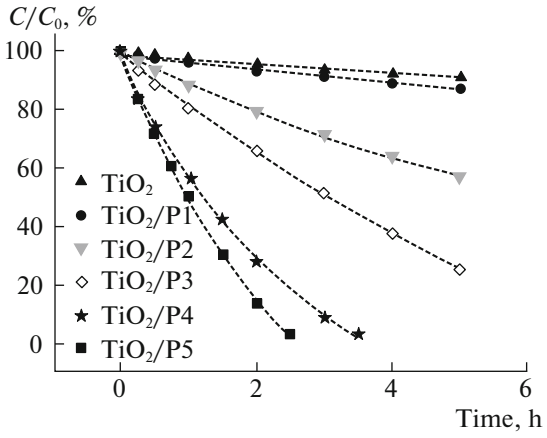

Fig. 4. Photocatalytic degradation of arylazo pyridone dye.

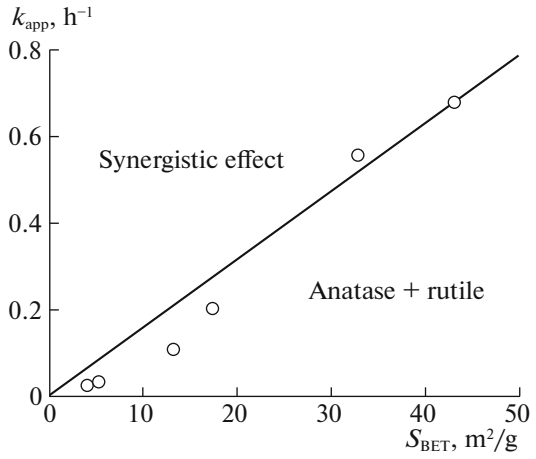

Fig. 5. Effect of surface area on reaction rate constant.

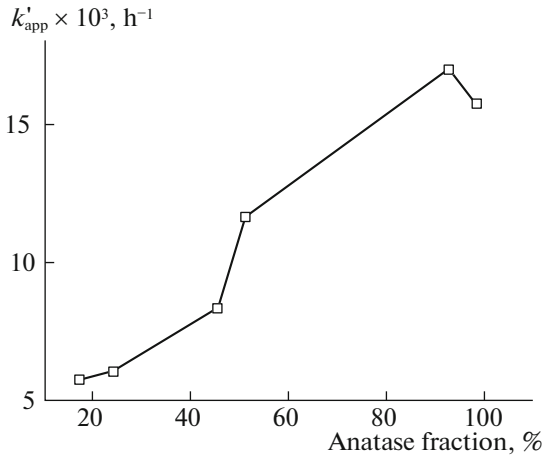

Fig. 6. Effect of anatase content on specific reaction rate constant.

were determined from the obtained kinetic curves and used as a measure of photocatalytic activity (table).

The obtained results clearly indicate that photoactivity of modified catalysts is significantly higher compared to control TiO_2. Among modified catalysts, TiO_2/P1 catalyst prepared with the lowest PEG content displayed the lowest activity. By increasing amount of PEG template, the photoactivity of the samples gradually increases and the highest photoactivity is observed for the sample TiO_2/P5.

Relationship between specific surface area and determined rate constant showed good positive linear correlation, implying that the degradation rate is mostly influenced by the surface area (Fig. 5).

In order to identify other factors that likely contribute to photoactivity enhancement, a more quantitative approach was made by presenting the rate constant per unit surface area (k'_{app}). The results revealed that with increasing molar ratio [PEG]/[TTIP] from 0.5 (sample TiO_2/P1) to 3 (sample TiO_2/P4) specific rate constant k'_{app} linearly increases. Further increase in molar ratio beyond optimal value led to small drop in k'_{app}. Thus, the unit of the surface area within the sample TiO_2/P4 is more active than within TiO_2/P5, although later showed higher activity (table).

If the surface area was the sole factor responsible for the change in photocatalytic rate, then normalized rate constants per surface area k'_{app} would be equal for all catalysts. However, different rate constants suggest that other intrinsic material factors, such as crystallinity, anatase/rutile ratio, light utilization, etc. may participate in photoactivity enhancement.

Correlation between specific constant per surface area and anatase fraction is presented in Fig. 6. The optimal anatase fraction is found to be about 90%, and further increase in anatase content does not improve photoactivity (Fig. 6). The obtained result is in accordance with some previous relevant works in the field, where mixture of anatase and rutile TiO_2 nanoparticles displayed much higher photoactivity than pure anatase form [18, 19]. The increased activity of mixed phase could be a consequence of synergistic effect between these two phases.

If anatase phase was the only phase responsible for catalyst activity, then rate constant per unit of anatase surface would be equal for all catalysts. However, the unit of anatase phase was the most active within the sample containing the lowest fraction of anatase and vice verse. This clearly indicates that either pure rutile phase is photoactive or that synergistic effect between anatase and rutile phase enhances the photoactivity.

Synergistic effect between anatase and rutile TiO_2 exists when the unit of TiO_2 surface area is more active then the unit of the surface of pure anatase phase. Figure 5 is divided in two sections by a line representing the activity of pure anatase. The area below the line represents overall activity of anatase and rutile phases, while the area above the line presents TiO_2 activity as a consequence of synergistic effect between anatase and rutile phases. The evidence of synergistic effect has been demonstrated only for TiO_2/P4 catalyst, which showed higher activity per unit of surface area compared to the pure anatase.

CONCLUSION

In this work TiO_2 photocatalysts were prepared by sol–gel process using different amounts of PEG as a template agent. The addition of PEGs affected not only porous and optical properties of the TiO_2 material, but also suppressed anatase to rutile transformation. The specific surface area and anatase fraction were found to be the most contributing factors for enhanced photoactivity. The TiO_2/P5 catalyst having

the highest surface area and consisting solely of anatase phase exhibited the highest activity. On the other hand, the unit of the surface area is more active within the TiO_2/P4 sample than within TiO_2/P5, which is evidence of synergistic effect between anatase and rutile phase. The main contribution of this study is to show that textural and structural properties of the material could be efficiently control with the small variation of PEG content.

ACKNOWLEDGMENTS

This work was supported by the Ministry of Education, Science and Technological Development of the Republic of Serbia (project no. III 45001). The authors wish to express their thanks to Dr. Zoran Vujičić from Instituto de Telecomunicações Universidade de Aveiro, Campus Universitário Aveiro, Portugal for constructive and helpful comments.

REFERENCES

1. A. Fujishima and K. Honda, Nature **238** (5358), 37 (1972).
2. K. Kato, A. Tsuzuki, H. Taoda, et al., J. Mater. Sci. **29**, 5911 (1994).
3. R. R. Bacsa and J. Kiwi, Appl. Catal. B: Environ. **16**, 19 (1998).
4. S. Bakardjieva, J. Subrt, V. Stengl, et al., Solid State Phenom. **90–91,** 7 (2003).
5. J. M. Calderon-Moreno, S. Preda, L. Predoana, et al., Ceram. Int. **40**, 2209 (2014).
6. S. Bu, Z. Jin, X. Liu, et al., Mater. Chem. Phys. **88**, 273 (2004).
7. W. Sun, S. Zhang, Z. Liu, et al., Int. J. Hydrogen Energ. **33**, 1112 (2008).
8. L. Wu, J. C. Yu, X. Wang, et al., J. Solid State Chem. **178**, 321 (2005).
9. Z. Peng, Z. Shi, and M. Liu, Chem. Commun. **21**, 2125 (2000).
10. H. Li, Y. Zhou, C. Lv, et al., Mater. Lett. **65**, 1808 (2011).
11. K-F. Du, J. Liu, X. Cui, et al., J. Sol–Gel Sci. Technol. **65**, 287 (2013).
12. E. P. Barrett, L. G. Joyner, and P. P. Halenda, J. Am. Chem. Soc. **73**, 373 (1951).
13. J. M. Dostanić, D. R. Lončarević, P. T. Banković, et al., J. Environ. Sci. Health, Part A **46**, 70 (2011).
14. H. Zhang and J. F. Banfield, Am. Mineral. **84**, 528 (1999).
15. R. L. Penn and J. F. Banfield, Am. Miner. **84**, 871 (1999).
16. G. H. Lee and J-M. Zuo, J. Am. Ceram. Soc. **87**, 473 (2004).
17. J. Tauc, R.Grigorovici, and A. Vancu, Phys. Status Solidi B **15**, 627 (1966)
18. R. I. Bickley, T. Gonzalez-Carreno, J. S. Lees, et al., J. Solid State Chem. **92**, 178 (1991).
19. D. C. Hurum, A. G. Agrios, and K. A. Gray, J. Phys. Chem. **107**, 4545 (2003).